Reactions of Laser-Ablated Boron Atoms with HCN during Condensation in Argon. A Comparison of Matrix Infrared and DFT, CCSD(T), and CASSCF Frequencies of BNC, BCN, HBNC, and HBCN

Dominick V. Lanzisera and Lester Andrews*

Department of Chemistry, University of Virginia, Charlottesville, Virginia 22901

Peter R. Taylor

Department of Chemistry and Biochemistry, University of California, San Diego, and San Diego Supercomputer Center, P.O. Box 85608, San Diego, California 92186-9784

Received: March 28, 1997; In Final Form: June 30, 1997[⊗]

Laser-ablated boron atoms (^{10}B, ^{11}B) have been reacted with hydrogen cyanide (HCN, $H^{13}CN$, DCN) during condensation in excess argon at 6−7 K. The major products observed in the matrix infrared spectrum are BNC and BCN with minor products HBNC, HBCN, and HB(CN). Although DFT calculations predict product vibrational frequencies reasonably well, CCSD(T) and CASSCF calculations are superior in predicting both frequencies and intensities. In particular, CCSD(T) calculations by Martin and Taylor of anharmonic frequencies for BNC correctly predicted the strong Fermi resonance interaction observed in the matrix spectrum.

Introduction

Matrix isolation studies of boron reactions with molecules containing carbon and/or nitrogen have resulted in the identification of several novel species with boron−carbon and/or boron−nitrogen bonds. Examples of such reactants include C_2H_2, CH_4, NH_3, and CH_3NH_2.[1−4] The CH_3NH_2 reaction produced three types of new products: those with B−C−N chains, those with B−N−C chains, and those with C−B−N chains.[4] These products exhibited similar spectral characteristics owing to their isoelectronic organic analogues with three carbons in a linear chain.

The most basic of boron/carbon/nitrogen species are BCN, BNC, and CBN. Thomson[5] carried out ab initio studies of BCN and BNC several years ago and determined energies and electronic structures of these species. Recently, Martin and Taylor[6] presented the results of CASSCF[7] and CCSD(T)[8] calculations on the structures and vibrational frequencies of BCN and BNC with comparison to isoelectronic C_3. The energy of CBN was shown to be much higher than that of the other boron/carbon/nitrogen molecules and not studied further. Since these calculations included anharmonicity, an interesting Fermi resonance was predicted in the C−N stretching region of BNC that harmonic methods cannot find. Because this Fermi resonance perturbed ^{10}BNC more than ^{11}BNC, the predicted isotopic splitting of the two was calculated to be 26.2 cm^{-1}, as opposed to 1.3 cm^{-1} in a harmonic calculation. In contrast, BCN had a calculated boron isotopic shift of 0.9 cm^{-1}, similar to that determined in the absence of Fermi resonance. Since BCN and BNC are unknown molecules, comparisons to experiment could not be performed. Using laser ablation combined with matrix isolation, however, it is possible to generate BCN and BNC, trap them in solid argon, and record infrared spectra of these molecules. In this article, we present such spectra following reactions of laser-ablated boron atoms with HCN for several isotopic combinations of boron, carbon, and hydrogen. The products HBNC, HBCN, and HB(CN) are observed and discussed as well.

Experimental Section

The apparatus for pulsed laser ablation, matrix isolation, and FTIR spectroscopy has been described previously.[1−4] Mixtures of 0.3% HCN, $H^{13}CN$, or DCN in Ar co-deposited at 3 mmol/h for 2 h onto a 6−7 K cesium iodide window reacted with boron atoms ablated from a target source rotating at 1 rpm. The fundamental 1064 nm beam of a Nd:YAG laser (Spectra Physics DCR-11) operating at 10 Hz and focused with a focal length = +10 cm lens ablated the target using 20−30 mJ/10 ns pulse. The procedure for preparing HCN was as reported.[9] For DCN, D_2SO_4 (Aldrich) and D_2O (Aldrich) were added to solid KCN (Aldrich), and because of prior HCN passivation of the manifold, the H/D ratio was near unity. For $H^{13}CN$, concentrated HCl was added to $K^{13}CN$ (Cambridge Isotope Laboratories) and a ^{13}C enrichment of greater than 80% was obtained. Two samples of boron were employed: natural boron ^{n}B (Aldrich, 80.4% ^{11}B, 19.6% ^{10}B) and ^{10}B (93.8%, Eagle Pitcher Ind.). Following deposition, a Nicolet 550 Fourier transform infrared (FTIR) spectrometer collected infrared spectra from 4000 to 400 cm^{-1} using a liquid nitrogen cooled MCT detector. The spectral resolution was 0.5 cm^{-1} with an accuracy of ±0.2 cm^{-1}. After sample deposition, annealing to 15 K followed by broadband mercury arc photolysis (Philips 175 W, 240−580 nm) produced changes in the FTIR spectra. Further annealings to 25 and 35 K also changed some of the spectral features.

Density functional theory (DFT) calculations were performed on potential product molecules using the Gaussian 94 program package.[10] All calculations used the B3LYP functional,[11] and the basis set for each atom was Dunning/Huzinaga full double-ζ with one single first polarization function (D95*).[12] The geometry optimizations used redundant internal coordinates and converged via the Berny optimization algorithm,[10,13] and the program calculated vibrational frequencies analytically. These inexpensive DFT calculations provided a simple guide to the possible product molecules. Afterward, higher order CASSCF (13 × 13) calculations were performed on HBNC, HBCN, and HB(CN) to complement previous calculations on BNC and BCN.[6]

[⊗] Abstract published in *Advance ACS Abstracts,* August 15, 1997.

S1089-5639(97)01116-X CCC: $14.00

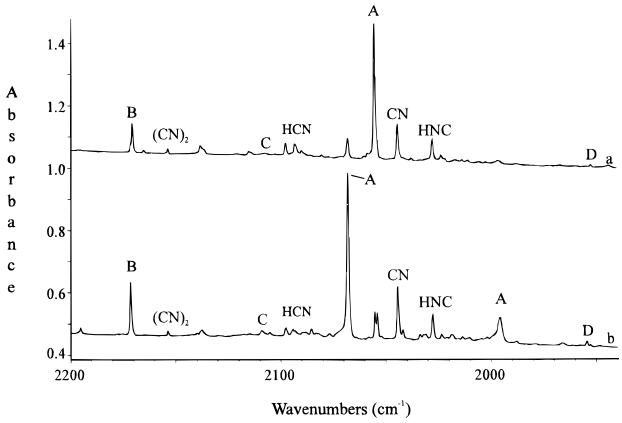

Figure 1. Matrix infrared spectra in the 2200−1940 cm^{-1} C≡N stretching region following pulsed laser ablation of B atoms co-deposited with Ar/HCN (300/1) samples on a CsI window at 6−7 K. (a) $^{n}B + H^{12}CN$ and (b) $^{10}B + H^{12}CN$.

Results

Matrix infrared spectra for various isotopic combinations are reported as well as the relative change in intensity of product peaks following broadband photolysis and subsequent annealing to 25 K. Besides the boron product peaks mentioned in this section, we observed bands for HNC, CN, and $(CN)_2$, all apparently formed by radiation from the ablation process. Also, boron oxides, such as BO, BO_2^-, $(BO)_2$, BO_2, and BOB are formed in trace quantities[14] from both oxides on the target surface and reaction of boron with residual H_2O or D_2O from the synthesis of HCN or DCN.

B + $H^{12}CN$. Figure 1 presents the spectra in the C≡N stretching region for reactions of ^{n}B (Figure 1a) and ^{10}B (Figure 1b) with naturally isotopic $H^{12}CN$. Common peaks to both spectra include HNC at 2027.5 cm^{-1}, CN at 2044.3 cm^{-1}, and $(CN)_2$ at 2153.8 cm^{-1}.[15,16] Table 1 lists all of the observed product bands in the experiment for the various isotopic combinations, as well as photolysis and annealing behavior. The strongest absorption in the ^{n}B spectrum, at 2055.2 cm^{-1} (labeled A) grows 30% on photolysis and decreases 30% on annealing to 25 K. A potential ^{10}B counterpart at 2068.0 cm^{-1} (also labeled A) tracks with this band and is the largest band in the ^{10}B spectrum. The next strongest product band in the ^{n}B experiment, at 2170.8 cm^{-1} (labeled B), has a blue shoulder at 2171.5 cm^{-1}. For the ^{10}B experiment, the 2171.5 cm^{-1} band (labeled B) dominates and decreases 30% on photolysis and 20% on 25 K annealing. A weaker ^{n}B absorption at 1952.2 cm^{-1} (labeled D) similarly tracks with a ^{10}B absorption at 1954.4 cm^{-1}. An even weaker tracking pair at 2108.0 and 2109.3 cm^{-1} (both labeled C) increases 130% on photolysis and decreases 30% on annealing. Finally, an absorption at 1995.8 cm^{-1} (labeled A) in the ^{10}B experiment has no observable ^{11}B counterpart in the ^{n}B experiment.

Although the C−H and N−H stretching regions show no new products, there are a few new bands in the B−H stretching region (Figure 2). The sharpest of these peaks, at 2708.6 cm^{-1} (labeled E) in the ^{n}B experiment has a counterpart one-fourth the size at 2725.3 cm^{-1}, which is the dominant new absorption in the ^{10}B spectrum. Both absorptions are completely destroyed on photolysis. By contrast, a ^{11}B absorption at 2664.8 cm^{-1} and the corresponding ^{10}B absorption at 2677.0 cm^{-1} (labeled C) both increase 130% on photolysis, followed by a 30% decrease on annealing. A weaker band at 2640.7 cm^{-1} in the ^{10}B experiment (labeled D) does not have any observable ^{11}B counterpart because it is masked by residual DCN.

In the lower frequency region (Figure 3), several product peaks are observed, including those of B_2N.[3,17] The largest of these (labeled A) at 984.3 and 1016.6 cm^{-1} in the ^{n}B and ^{10}B experiments, respectively, track with each other and have the same absorption profile. A ^{10}B absorption at 826.2 cm^{-1} (labeled B) has a ^{11}B counterpart at 800.0 cm^{-1}, which is slightly obscured in the ^{n}B experiment by a nearby HCN cluster absorption. The moderately intense 1081.0 and 1108.6 cm^{-1} peaks (labeled E) disappear on photolysis. A similarly intense ^{10}B absorption at 748.1 cm^{-1} (labeled E) has a ^{11}B counterpart at 736.8 cm^{-1}, on the shoulder of a HCN matrix site absorption, with broadband photolysis destroying both bands. A pair of bands at 938.4 and 964.3 cm^{-1} have similar absorption profiles and track with each other and are labeled C. Weaker bands at 1046.4 and 1077.0 cm^{-1} behave similarly and are labeled D.

B + $H^{13}CN$. The C≡N stretching region for experiments with isotopically enriched carbon is presented in Figure 4. Because the ^{13}C enrichment was less than 100%, some bands from the ^{12}C experiments can be observed. Although not in the 4:1 ratio expected for boron products in a ^{n}B experiment, peaks at 2021.6 and 2039.6 cm^{-1} form a boron isotopic doublet and track with the peaks labeled A for ^{12}C, which are also observed in Figure 4. The next largest peaks, at 2122.1 and 2122.8 cm^{-1}, similarly track with the absorptions labeled B in Figure 1. Matches for the ^{12}C peaks labeled D can be found at 1919.2 and 1920.9 cm^{-1} for ^{11}B and ^{10}B, respectively. Weak absorptions at 2057.0 and 2062.3 cm^{-1} show a large increase on photolysis and moderate decrease on annealing, apparently tracking with the C bands from the ^{12}C experiments, but these bands are too weak to make such an assignment definitive. Finally, an absorption at 1972.4 cm^{-1} (labeled A) with ^{10}B has no observable ^{11}B counterpart.

The B−C/N stretching region of the B + $H^{13}CN$ spectrum (Figure 5) exhibits features similar to those of Figure 3, but shifted in frequency with the exception of B_2N for obvious reasons. The pair of peaks at 976.1 and 1008.2 cm^{-1} shifts slightly more than 8 cm^{-1} from their ^{12}C counterparts (see Table 1). Similarly, absorptions at 796.0 and 822.4 cm^{-1} are only 4 cm^{-1} shifted in the $H^{13}CN$ experiments. Other boron doublet peaks with small shifts from their ^{12}C counterparts include 1075.6/1102.9 cm^{-1} (5−6 cm^{-1} shift), 1037.1/1068.0 cm^{-1} (9 cm^{-1}), 934.2/960.7 cm^{-1} (4−6 cm^{-1}), and 725.9/737.7 cm^{-1} (11 cm^{-1}).

In the B−H stretching region, ^{13}C shifts are much smaller, as expected. The 2664.8/2677.0 cm^{-1} boron doublet (labeled C) from the $H^{12}CN$ experiments shows no observable shift in the ^{13}C experiments. Similarly, the ^{10}B product peak at 2640.7 cm^{-1} does not shift, either. The pair labeled E, however, shifts to 2708.3/2722.9 cm^{-1}, and the 2.4 cm^{-1} carbon isotopic shift for the ^{10}B product is very unusual.

B + DCN. Because the synthesis of DCN yielded some HCN as well, products from B + HCN experiments appeared in B + DCN spectra, albeit at lower yields. Other products had comparable yields regardless of the sample deuteration, which identified products without hydrogen atoms. The two largest pairs of new peaks from Figure 1, labeled A and B, remained intense in the DCN experiments. Also present in this region of the spectrum are B−D absorptions. A tracking pair at 2037.9 and 2042.0 cm^{-1} disappears on photolysis and must be the deuterated counterpart of the 2708.6/2725.3 cm^{-1} pair from the HCN experiments. Similarly, a boron doublet at 1971.2/1989.6 cm^{-1} grows enormously on photolysis and has the same broadband profile as the 2664.8/2677.0 cm^{-1} B−H stretches in Figure 2.

TABLE 1: Observed Frequencies (cm^{-1}) for Products of Boron−Hydrogen Cyanide Reactions

10/12/1[a]	11\12\1[a]	10/13/1[a]	11/13/1[a]	10/12/2[a]	11/12/2[a]	phot/ann[b]	identity
2725.3	2708.6	2722.9	2708.3	2042.0	2037.9	−100/−	HB(CN)
2677.0	2664.8	2677.0	2664.8	1989.6	1971.2	+130/−30	HBCN
2667.3	2654.0	2667.3	2654.0			+130/−30	HBCN site
2640.7		2640.7				+90/+20	HBNC?
2306.9	2298.3	2306.9	2298.3	1721.1	1708.5	+5/−25	(H_2)BH
2268.3	2259.4	2268.3	2259.4	1695.2	1682.6	+10/−35	BH
2195.3	2165.2	2181.0	2144.6			+40/+15	?
2171.5	2170.8	2122.8	2122.1	2171.5	2170.8	−30/−20	BCN
2153.8	2153.8	2091.2	2091.2	2153.8	2153.8	+15/−20	$(CN)_2$
2109.3	2108.0	2062.3[c]	2057.0[c]			+130/−30	HBCN
2085.4	2080.5					+150/+25	?
2068.0	2055.2	2039.6	2021.6	2068.0	2055.2	+30/−30	BNC
2044.3	2044.3	2002.0	2002.0	2044.3	2044.3	−5/−30	CN
1995.8		1972.4		1995.8		+30/−30	BNC
1954.4	1952.2	1920.9	1919.2			+90/+20	HBNC
1769.1	1736.4	1769.1	1736.4	1769.1	1736.4	−100/−	BNB
1261.7	1225.1	1256.5	1221.2			+120/0	?
1108.6	1081.0	1102.9	1075.6	1062.6	1042.7	−100/−	HB(CN)
1077.0	1046.4	1068.0	1037.1	1056.4	1024.7	+90/+20	HBNC
1016.6	984.3	1008.2	976.1	1016.6	984.3	+30/−30	BNC
964.6	938.4	960.7	934.2	931.2	908.6	+130/−30	HBCN
901.5	882.1	901.5	882.1	901.5	882.1	0/−15	B_2N
826.2	800.0	822.4	796.0	826.2	800.0	−30/−20	BCN
748.1	736.8	737.7	725.9	748.2?	737.4?	−100/−	HB(CN)
				618.6	607.3	+15/−45	?

[a] Isotopes for boron/carbon/hydrogen. [b] Percent increase or decrease on photolysis/annealing to 25 K. [c] Tentative assignment.

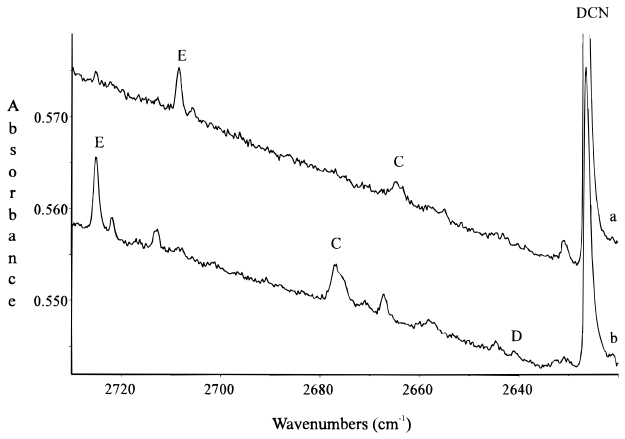

Figure 2. Matrix infrared spectra in the 2730−2620 cm^{-1} B−H stretching region following pulsed laser ablation of B atoms co-deposited with Ar/HCN (300/1) samples on a CsI window at 6−7 K. (a) $^{n}B + H^{12}CN$ and (b) $^{10}B + H^{12}CN$.

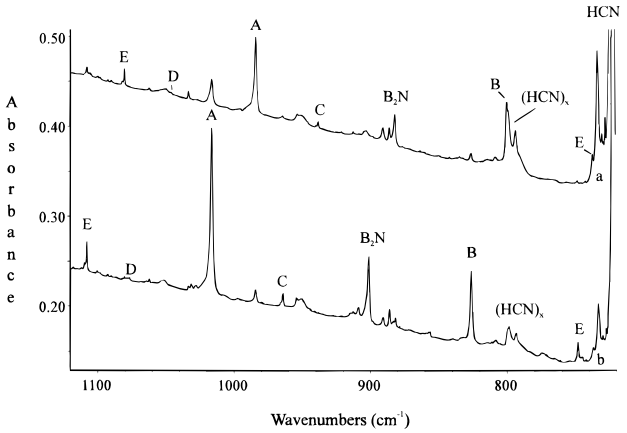

Figure 3. Matrix infrared spectra in the 1120−720 cm^{-1} B−N and B−C stretching regions following pulsed laser ablation of B atoms co-deposited with Ar/HCN (300/1) samples on a CsI window at 6−7 K. (a) $^{n}B + H^{12}CN$ and (b) $^{10}B + H^{12}CN$.

Figure 6 presents the spectrum from 1120 to 720 cm^{-1}, the region for B−C and B−N stretching absorptions. A few peaks from the HCN experiments are present in these spectra, including those of B_2N. The 984.3/1016.6 cm^{-1} and 800.0/826.2 cm^{-1} pairs are of intensity comparable to those of Figure 3. The 1081.0/1108.6 cm^{-1} peaks are much smaller than in Figure 3, but to the red of them is a boron doublet with the same band profiles at 1042.7 and 1062.6 cm^{-1}, also destroyed upon photolysis. Near these peaks are weaker bands at 1024.7 and 1056.4 cm^{-1} which track with the bands labeled D from the $H^{12}CN$ experiments. Also, absorptions at 908.6 and 931.2 cm^{-1} are shifted approximately 30 cm^{-1} from their natural isotopic counterparts (see Table 1).

Calculations. DFT/B3LYP calculations on all isomers of BCN and HBCN are provided in Table 2. Although this method treats dynamical and nondynamical correlation less elaborately than CCSD(T) and CASSCF calculations, respectively, it is reliable enough to confirm that CBN and the other cyclic species, HCNB and HNCB, are not energetically feasible. Table 3 presents CASSCF calculations on the products of this reaction and includes energies, geometries, and vibrational frequencies with intensities. Harmonic frequencies and isotope shifts at the CASSCF level were obtained from analytical second derivatives using the DALTON program.[18] The CASSCF active space comprised all valence orbitals on H, B, C, and N: a 13 electrons in 13 orbitals treatment; the basis set used was Dunning's correlation-consistent polarized valence double-ζ set.[19] All HBCN isomers treated have a plane of symmetry, and the ground electronic states are $^2A'$. This is perhaps best regarded as derived from the $^3\Pi$ excited state of BNC (or BCN) where the hydrogen forms a two-electron bond to the boron atom using one of the open-shell orbitals of BNC (or BCN).

We have noted in previous work that although the absolute accuracy of CASSCF vibrational frequencies is only fair (stretching frequencies are typically underestimated by about 5%), the isotopic shifts are very accurate indeed, certainly accurate enough to provide fingerprint identifications in previous work on B/C/H systems.[20] We can be confident that the same holds true for the present work, unless there are very significant difficulties with resonances.[7,8]

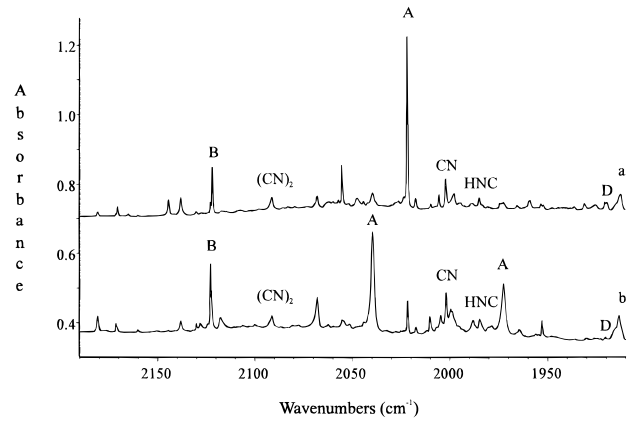

Figure 4. Matrix infrared spectra in the 2190−1910 cm^{-1} C≡N stretching region following pulsed laser ablation of B atoms co-deposited with Ar/H^{13}CN (300/1) samples on a CsI window at 6−7 K. (a) ^{n}B + H^{13}CN and (b) ^{10}B + H^{13}CN.

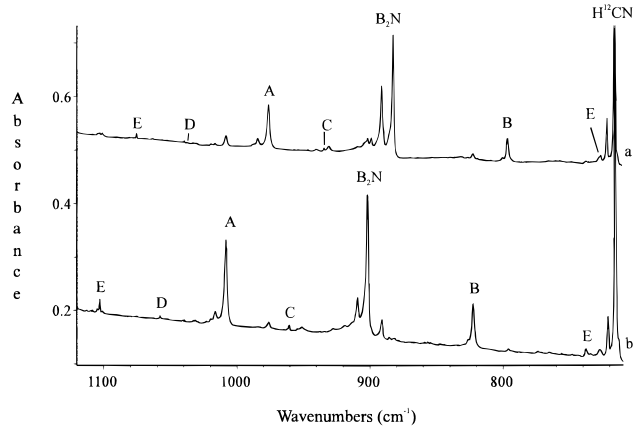

Figure 5. Matrix infrared spectra in the 1120−710 cm^{-1} B−N and B−C stretching regions following pulsed laser ablation of B atoms co-deposited with Ar/H^{13}CN (300/1) samples on a CsI window at 6−7 K. (a) ^{n}B + H^{13}CN and (b) ^{10}B + H^{13}CN.

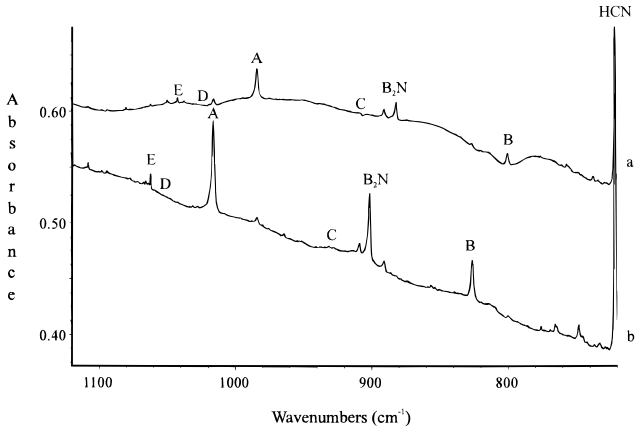

Figure 6. Matrix infrared spectra in the 1120−720 cm^{-1} B−N and B−C stretching regions following pulsed laser ablation of B atoms co-deposited with Ar/DCN (300/1) samples on a CsI window at 6−7 K. (a) ^{n}B + DCN and (b) ^{10}B + DCN.

Discussion

By comparing the photolysis and annealing behavior of product absorptions, one can group a number of bands and assign them to the same product. With the aid of CASSCF and CCSD calculations and to a lesser extent DFT calculations and observed isotopic shifts, these species can be identified.

Species A: BNC. The strong 2055.2 and 984.3 cm^{-1} absorptions increase 30% on photolysis and decrease 30% on annealing to 25 K. The ^{10}B−^{11}B pattern in the ^{n}B experiments is appropriate for a single B atom absorber, and agreement with CCSD(T) frequency calculations substantiates assignment of these bands to BNC. Experimental and calculated frequencies for BNC are provided in Table 4. Martin and Taylor predicted a Fermi resonance in this molecule arising from the coupling of the C≡N stretching mode with the first overtone of the B−N stretch. When the deperturbed upper band does not shift much with different boron isotopes (as in a C≡N stretch), the coupling overtone band has a large boron shift (as in a B−N stretch), and the perturbation on the upper band will depend on the isotope of boron. For BNC, the ^{10}B−N overtone more closely matches the C≡N stretch and pushes it higher in frequency than does the ^{11}B−N overtone. The result is a C≡N stretch with a 12.8 cm^{-1} boron isotopic shift for the ^{12}C and a 18.0 cm^{-1} shift for the ^{13}C-substituted molecules. Another result of the Fermi resonance is that the 2068.0 cm^{-1} absorption is less than one-fourth that of the 2055.2 cm^{-1} peak in the ^{n}B spectrum, while the overtone absorption appears for the ^{10}BN^{12}C product at 1995.8 cm^{-1} but not for the ^{11}BN^{12}C product. This is even more pronounced for ^{10}BN^{13}C where intensity is shared more between the fundamental and overtone (1972.4 cm^{-1}). The mixing of the two modes in ^{10}BNC increases the intensity of the overtone band at the expense of the C≡N fundamental intensity. Note that the Fermi resonance is stronger for ^{10}BN^{13}C than ^{10}BN^{12}C as attested by the relative strengths of the overtone and fundamental (1−2 for ^{10}BN^{13}C and 1−7 for ^{10}BN^{12}C; see Figures 1 and 4).

The CCSD calculations predict higher frequencies and a larger boron isotope shift than is observed, but the Fermi resonance complicates such calculations—small deviations in the B−N overtone and the deperturbed C≡N fundamental can effect a larger difference in calculations of the perturbed C≡N fundamental. The observed/calculated ratios are the same for the B−N stretching mode but differ slightly for the C≡N mode because of Fermi resonance. The ratios all agree for BCN, which has no Fermi resonance.

The CCSD calculations give the B−N stretching fundamentals within 7 cm^{-1} (i.e., less than 1%) of the observed values for both boron isotopes. That the 984.3/1016.6 cm^{-1} pair (976.1/1008.2 cm^{-1} for BN^{13}C) track with the C≡N stretch in relative intensity on photolysis and annealing confirms this assignment. The bending mode, predicted at less than 200 cm^{-1}, cannot be observed with the present instrumentation.

Note that calling the 984.3/1016.6 cm^{-1} pair "B−N stretching modes" is an oversimplification. Such modes would have no carbon-13 shift, but in fact 8.2 and 8.4 cm^{-1} carbon-13 shifts are found here. The observed 10/11 ratio is 1.0328, which is higher than the 1.0275 ratio calculated for diatomic B−N. Clearly, this lower frequency stretching mode, which involves B and C more than a diatomic B−N stretching mode, has some "symmetric" B−N−C stretching character.

Species B: BCN. The medium-intensity bands at 2170.8 and 800.0 cm^{-1} decrease 30% on photolysis and are assigned to BCN. As with BNC, the calculations predict two observable stretching modes and a bending mode beyond the range of the instrument. Experimental and calculated frequencies are presented in Table 4. CCSD calculations for the C≡N stretch predict a small 0.9 cm^{-1} boron isotopic shift for B^{12}CN and the ^{11}B/^{10}B peaks observed at 2171.5/2170.8 cm^{-1} match the calculations extremely well. Without a Fermi resonance to complicate matters, such calculations are nearly perfect when predicting the observed vibrational frequencies. Despite the Fermi resonance in BNC which perturbs the C≡N frequencies higher, the C≡N stretch of BCN is still more than 100 cm^{-1}

TABLE 2: DFT/B3LYP Calculations for Potential Products from Reactions of B with HCN

species	energy (au)	bond lengths (Å)	bond angles (deg)	frequencies[a] in cm^{-1} (intensities in km mol^{-1})
HBCN	−118.215 17	$r_{HB} = 1.18$; $r_{BC} = 1.48$; $r_{CN} = 1.18$	$\angle_{HBC} = 138.9$; $\angle_{BCN} = 174.2$	2797.5(32), 2155.7(9), 972.7(32), 599.6(14), 353.8(6), 297.9(5)
HBNC	−118.215 16	$r_{HB} = 1.18$; $r_{BN} = 1.39$; $r_{NC} = 1.20$	$\angle_{HBN} = 130.9$; $\angle_{BNC} = 175.5$	2736.9(64), 1987.7(88), 1097.8(15), 759.0(32), 349.0(4), 284.8(4)
HB(CN)	−118.208 00	$r_{HB} = 1.17$; $r_{BC} = 1.54$; $r_{CN} = 1.28$; $r_{BN} = 1.44$	$\angle_{HBC} = 161.0$; $\angle_{BCN} = 60.7$; $\angle_{BNC} = 68.6$; $\angle_{HBN} = 148.3$	2847.4(33), 1655.1(22), 1123.0(53), 776.2(18), 724.1(43), 674.5(7)
HC(NB)	−118.183 43	$r_{HC} = 1.09$; $r_{CN} = 1.32$; $r_{NB} = 1.44$; $r_{BC} = 1.46$	$\angle_{HCN} = 129.9$; $\angle_{HCB} = 168.2$; $\angle_{BNC} = 63.8$; $\angle_{BCN} = 61.9$	3184.2(5), 1544.2(15), 1226.2(3), 1129.1(53), 908.2(28), 892.1(8)
HN(CB)	−118.131 50	$r_{HN} = 1.03$; $r_{NC} = 1.37$; $r_{BC} = 1.59$; $r_{NB} = 1.39$	$\angle_{HNC} = 131.1$; $\angle_{BCN} = 55.4$; $\angle_{HNB} = 158.8$; $\angle_{CNB} = 70.1$	3448.9(9), 1412.6(11), 1214.5(133), 959.8(14), 842.6(17), 814.0(56)
BNC	−117.584 73	$r_{BN} = 1.43$; $r_{NC} = 1.20$	$\angle_{BNC} = 180.0$	2115.0(687), 1012.0(201), 220.3(19×2)
BCN	−117.564 41	$r_{BC} = 1.60$; $r_{CN} = 1.17$	$\angle_{BCN} = 180.0$	2262.5(201), 800.8(234), 192.5(28×2)
CBN	−117.459 68	$r_{CB} = 1.46$; $r_{BN} = 1.29$	$\angle_{CBN} = 180.0$	1964.3(315), 983.3(40), 128.1(32×2)

[a] For ^{11}B, ^{1}H, and ^{12}C.

TABLE 3: CASSCF Calculations for Potential Products from Reactions of B with HCN

species	energy (au)	bond lengths (Å)	bond angles (deg)	frequencies[a] in cm^{-1} (intensities in km mol^{-1})
HBCN	−117.689 25	$r_{HB} = 1.21$; $r_{BC} = 1.53$; $r_{CN} = 1.19$	$\angle_{HBC} = 129.1$; $\angle_{BCN} = 175.9$	2631.4(72), 2157.9(44), 907.5(40), 783.0(40), 328.6(4), 280.2(6)
HBNC	−117.686 80	$r_{HB} = 1.21$; $r_{BN} = 1.42$; $r_{NC} = 1.21$	$\angle_{HBN} = 125.2$; $\angle_{BNC} = 174.9$	2598.6(106), 2023.4(254), 1024.6(60), 891.7(25), 281.5(1), 207.9(2)
HB(CN)	−117.672 25	$r_{HB} = 1.18$; $r_{BC} = 1.54$; $r_{CN} = 1.29$; $r_{BN} = 1.46$	$\angle_{HBC} = 163.2$; $\angle_{BCN} = 61.2$; $\angle_{BNC} = 68.1$; $\angle_{HBN} = 146.1$	2905.7(48), 1612.9(19), 1087.6(53), 759.8(47), 707.9(6), 809.7(23)
BNC[b]	−117.095 18	$r_{BN} = 1.46$; $r_{NC} = 1.18$	$\angle_{BNC} = 180.0$	2073(666), 966(245), 187(11×2)
BCN[b]	−117.564 41	$r_{BC} = 1.59$; $r_{CN} = 1.18$	$\angle_{BCN} = 180.0$	2073(172), 842(211), 187(18×2)

[a] Frequencies for ^{11}B, ^{1}H, and ^{12}C. [b] Reference 6.

TABLE 4: Observed and Calculated Vibrational Frequencies (cm^{-1}) for BNC and BNC Using B3LYP (Harmonic) and CCSD (Anharmonic)[a]

BNC	11−14−12	10−14−12	11−14−13	10−14−13	assign
obs	2055.2	2068.0	2021.6	2039.6	ν_1
B3LYP	2115.0	2116.8	2078.5	2080.5	
CCSD	2076.0	2102.2			
obs		1995.8		1972.4	$2\nu_2$
obs	984.3	1016.6	976.1	1008.2	ν_2
B3LYP	1012.0	1045.9	1002.6	1034.4	
CCSD	991.0	1023.0			

BNC	11−12−14	10−12−14	11−13−14	10−13−14	assign
obs	2170.8	2171.5	2122.1	2122.8	ν_1
B3LYP	2262.5	2263.5	2210.8	2211.5	
CCSD	2165.5	2166.4			
obs	800.0	826.2	796.0	822.4	ν_2
B3LYP	800.8	828.0	797.9	825.3	
CCSD	809.9	836.4			

[a] CCSD (anharmonic) calculations from ref 6.

higher than that of BNC, indicating stronger C≡N triple-bond character in BCN.

Calculated frequencies for the lower frequency stretching mode are also in excellent agreement with experiment. The 800.0/826.2 cm^{-1} absorptions are both only 1.2% lower than those calculated for BCN. The ^{13}C shifts of these peaks are 4.0 and 3.8 cm^{-1}, which are actually one-half that of the low-frequency stretch of BNC. The small carbon-13 shifts result from the symmetric stretching character of this mode with little carbon motion. Accordingly, this mode also involves boron more (10/11 ratio 1.0328) than a diatomic B−C motion (calculated harmonic ratio 1.0256). The analogous mode in BNC involves more carbon motion and gives more carbon isotopic shift than in BCN.

The decrease of BCN and growth of BNC on photolysis suggests a photochemical rearrangement to the more stable isomer. The ultraviolet light apparently provides sufficient energy to overcome the activation barrier for conversion of BCN to BNC.

Species C−E: HBCN Isomers. Unlike those of BNC and BCN, the other new product bands in the B + HCN experiments show a marked decrease in the B + DCN experiments. The most obvious candidates for new products are the insertion product HBCN and the rearrangement isomer HBNC. No new products with two boron (i.e., no isotopic triplets or quartets in the ^{n}B spectra) or two carbon atoms could be observed, thereby limiting the possible identities of these products. Because two or three distinct B−H and no new observable C−H or N−H stretching modes appeared, all other new products must have hydrogen bound to boron. These other product peaks can be grouped into three general categories: those that increase a great deal on photolysis and decline on 25 K annealing, those that are destroyed on photolysis, and those that increase on both photolysis and annealing.

Tables 5 and 6 list the CASSCF vibrational frequencies of HBCN and HBNC, respectively, as well as the observed frequencies that best match them. The HBCN absorptions are marked by a greater than 2-fold increase in intensity upon photolysis and a decline on annealing to 25 K. HBNC absorptions also increase on photolysis, but to a lesser extent than those of HBCN. HBNC peaks grow upon annealing, further distinguishing them from HBCN bands. For each of these products, the B−H and C≡N stretching modes were identified, as well as the B−C or B−N stretching mode. Other predicted modes could not be observed in these experiments. Although the calculated intensities for these products are smaller than those of BCN and BNC, the observed intensities are far smaller than the BCN and BNC bands, which indicate that products with hydrogen are minor. Finally, the "C≡N" stretching mode of HBCN at 2109.3 cm^{-1} compares favorably with the "C≡C" stretching mode of the isoelectronic molecule HBCCH at 2080.4 cm^{-1}; both modes have small boron isotopic shifts.[1]

One remaining product has a strong B−H stretching mode and is destroyed on photolysis. Table 7 presents CASSCF calculations on the cyclic molecule HB(CN). These calculations predict a strong B−H stretch at 2905.7 cm^{-1} for natural isotopes,

TABLE 5: Experimental and CASSCF Vibrational Frequencies (cm^{-1}) for HBCN

	$H^{11}B^{12}CN$	$H^{10}B^{12}CN$	$H^{11}B^{13}CN$	$H^{10}B^{13}CN$	$D^{11}B^{12}CN$	$D^{10}B^{12}CN$
obsd	2664.8	2677.0	2664.8	2677.0	1971.2	1989.6
calcd	2631.4	2643.4	2631.3	2643.2	1942.7	1958.9
obsd	2108.0	2109.3	2057.0[a]	2062.3[a]		
calcd	2157.9	2158.5	2107.8	2108.5	2162.0	2164.0
obsd	938.4	964.6	934.2	960.7	908.6	931.2
calcd	907.5	935.8	904.2	932.7	892.1	918.5

[a] Tentative assignment.

TABLE 6: Experimental and CASSCF Vibrational Frequencies (cm^{-1}) for HBNC

	$H^{11}BN^{12}C$	$H^{10}BN^{12}C$	$H^{11}BN^{13}C$	$H^{10}BN^{13}C$	$D^{11}BN^{12}C$	$D^{10}BN^{12}C$
obsd		2640.7		2640.7		
calcd	2598.6	2610.4	2598.6	2610.4	2029.4	2033.5
obsd	1952.2	1954.4	1919.2	1920.9		
calcd	2023.4	2024.5	1988.0	1989.3	1917.0	1931.6
obsd	1046.4	1077.0	1037.1	1068.0	1024.7	1056.4
calcd	1024.6	1057.6	1015.7	1048.7	1010.1	1040.7

TABLE 7: Experimental and CASSCF Vibrational Frequencies (cm^{-1}) for Cyclic HB(CN)

	$H^{11}B(^{12}CN)$	$H^{10}B(^{12}CN)$	$H^{11}B^{13}CN$	$H^{10}B(^{13}CN)$	$D^{11}B(^{12}CN)$	$D^{10}B(^{12}CN)$
obsd	2708.6	2725.3	2708.3	2722.9	2037.9	2042.0
calcd	2905.7	2920.6	2905.7	2920.5	2173.2	2198.0
obsd	1081.0	1108.6	1075.6	1102.9	1042.7	1062.6
calcd	1087.6	1116.2	1078.8	1110.6	1046.3	1069.6
obsd	736.8	748.1	725.9	737.7	737.4?	748.2?
calcd	759.8	774.9	755.1	768.3	750.3	762.9

which is higher in energy than a typical B−H stretch. The predicted isotopic shift of 14.9 cm^{-1} is also larger than usual, suggesting that the 2725.3/2708.6 cm^{-1} pair of absorptions correspond to cyclic HB(CN). These calculations predict little to no isotopic carbon shift but do not take into account perturbations in the frequencies. Also predicted for ^{11}B are bands at 1612.0 and 1087.6 cm^{-1}, and the combination band should fall just below the B−H stretch, thereby perturbing the frequency of this stretch higher. We actually observe the predicted 1087.6 cm^{-1} band at 1081.0 cm^{-1}, and the other isotopes are in excellent agreement with the calculations. If the band predicted at 1612.9 cm^{-1} also nearly matches the calculations, then the combination band should fall near the B−H stretch. This Fermi resonance affects different isotopomers differently, as in BNC, and accounts for the carbon isotopic splitting observed in the spectra. Finally, the bending absorptions near 740 cm^{-1} also agree very well with the calculations. Thus, we are able to observe the three modes which CASSCF calculations predict to be the strongest.

Conclusions

Matrix isolation spectra of the products of the reaction of boron and hydrogen cyanide are reported. The main products are BNC and BCN, with minor products HBCN, HBNC, and HB(CN). The C≡N stretch of BNC is perturbed by a Fermi resonance of the overtone of the B−N stretching mode and is more pronounced for ^{10}BNC than for ^{11}BNC. No observed products had more than one carbon and one nitrogen atom, probably because of the low concentration of HCN in the Ar mixture. While DFT calculations come reasonably close to predicting vibrational frequencies, CCSD(T) and CASSCF are far superior in predicting both frequencies and intensities. In particular, recent CCSD(T) calculated anharmonic frequencies[6] are extremely close to the experimental frequencies reported here including Fermi resonance interaction in BNC.

Among the products, CCSD(T) calculations predict BNC to be only 9.5 kcal mol^{-1} more stable than BCN, and the B + HCN reaction produces both products in the matrix. The decrease of BCN and growth of BNC on broadband photolysis suggests a photochemical rearrangement of BCN to BNC. No CBN was observed in these experiments, and the calculated energies predict this molecule to be much less stable than the other linear isomers. The energies of HBCN and HBNC are very close to each other and only about 10 kcal mol^{-1} lower than that of the cyclic molecule, but the cyclic molecule HB(CN) converts to either HBNC or HBCN upon broadband photolysis. No evidence for other cyclic products was found in these experiments.

Acknowledgment. The experimental work was supported by the Air Force Office of Scientific Research. The $K^{13}CN$ sample was provided by Cambridge Isotope Laboratories. The computational work at SDSC was supported by the National Science Foundation under Grant No. CHE-9320718 and Cooperative Agreement No. DASC-8909825. The calculations at SDSC were performed on a HALstation model 330. P.R.T. acknowledges the assistance of L. Barnes and S. Christie of HAL Computer Systems, Inc. in arranging for the loan of this workstation.

References and Notes

(1) Andrews, L.; Hassanzadeh, P.; Martin, J. M. L.; Taylor, P. R. *J. Phys. Chem.* **1993**, *97*, 5839.
(2) Hassanzadeh, P.; Hannachi, Y.; Andrews, L. *J. Phys. Chem.* **1993**, *97*, 6418.
(3) Thompson, C. A.; Andrews, L. *J. Am. Chem. Soc.* **1995**, *117*, 10125. Thompson, C. A.; Andrews, L.; Martin, J. M. L.; El-Yazal, J. *J. Phys. Chem.* **1995**, *99*, 13839.
(4) Lanzisera, D. V.; Andrews, L. *J. Phys. Chem. A* **1997**, *101*, 824.
(5) Thomson, C. *J. Chem. Phys.* **1973**, *58*, 216.
(6) Martin, J. M. L.; Taylor, P. R. *J. Phys. Chem.* **1994**, *98*, 6105.
(7) Roos, B. O. *Adv. Chem. Phys.* **1987**, *69*, 399.
(8) Raghavachari, K.; Trucks, G. W.; Pople, J. A.; Head-Gordon, M. *Chem. Phys. Lett.* **1989**, *157*, 479.
(9) Bohn, R. B.; Andrews, L. *J. Phys. Chem.* **1989**, *93*, 3974.
(10) Gaussian 94, Revision B.1: Frisch, M. J.; Trucks, G. W.; Schlegel, H. B.; Gill, P. M. W.; Johnson, B. G.; Robb, M. A.; Cheeseman, J. R.; Keith, T.; Petersson, G. A.; Montgomery, J. A.; Raghavachari, K.; Al-Laham, M. A.; Zakrzewski, V. G.; Ortiz, J. V.; Foresman, J. B.; Cioslowski, J.; Stefanov, B. B.; Nanayakkara, A.; Challacombe, M.; Peng,

C. Y.; Ayala, P. Y.; Chen, W.; Wong, M. W.; Andres, J. L.; Replogle, E. S.; Gomperts, R.; Martin, R. L.; Fox, D. J.; Binkley, J. S.; Defrees, D. J.; Baker, J.; Stewart, J. P.; Head-Gordon, M.; Gonzalez, C.; Pople, J. A. Gaussian, Inc.: Pittsburgh, PA, 1995.

(11) Becke, A. D. *J. Chem. Phys.* **1993**, *98*, 5648.

(12) Dunning, T. H., Jr.; Hay, P. J. In *Modern Theoretical Chemistry*; Schaefer, H. G. III, Ed.; Plenum: New York, 1976; pp 1−28.

(13) Schlegel, H. B. *J. Comput. Chem.* **1982**, *3*, 214.

(14) Burkholder, T. R.; Andrews, L. *J. Chem. Phys.* **1991**, *95*, 8697. Andrews, L.; Burkholder, T. R. *J. Phys. Chem.* **1991**, *95*, 8554.

(15) Milligan, D. E.; Jacox, M. E. *J. Chem. Phys.* **1967**, *47*, 278.

(16) Hunt, R. D.; Andrews, L. *J. Phys. Chem*. **1987**, *91*, 5594.

(17) Hassanzadeh, P.; Andrews, L. *J. Phys. Chem.* **1992**, *96*, 9177.

(18) DALTON is an electronic structure program written by T. Helgaker, H. J. Aa. Jensen, P. Jörgensen, H. Koch, J. Olsen, H. Ågren, K. L. Bak, V. Bakken, O. Christiansen, P. Dahle, E. Dalskov, T. Enevoldsen, A. Halkier, H. Heiberg, D. Jonsson, R. Kobayashi, A. S. de Meras, K. V. Mikkelsen, P. Norman, M. J. Packer, B. J. Persson, K. Ruud, P. R. Taylor, and O. Vahtras.

(19) Dunning, T. H., Jr. *J. Chem. Phys.* **1989**, *90*, 1009.

(20) Martin, J. M. L.; Taylor, P. R.; Yustein, J. T.; Burkholder, T. R.; Andrews, L. *J. Chem. Phys*. **1993**, *99*, 12.